Author Manuscript

Author Manuscript

Author Manuscript

Author Manuscript

HHS Public Access

Author manuscript

J Biomech. Author manuscript; available in PMC 2021 June 07.

Published in final edited form as:

J Biomech. 2021 May 07; 120: 110367. doi:10.1016/j.jbiomech.2021.110367.

Simulation of preoperative flexion contracture in a computational model of total knee arthroplasty: Development and evaluation

Shady S. Elmasry[a,b,*], **Brian P. Chalmers**[c], **Cynthia A. Kahlenberg**[c], **David J. Mayman**[c], **Timothy M. Wright**[a], **Geoffrey H. Westrich**[c], **Michael B. Cross**[c], **Peter K. Sculco**[c], **Carl W. Imhauser**[a]

[a]Department of Biomechanics, Hospital for Special Surgery, Weill Cornell Medicine of Cornell University, New York, NY, USA

[b]Department of Mechanical Design and Production, Faculty of Engineering, Cairo University, Egypt

[c]Department of Orthopedic Surgery, Hospital for Special Surgery, Weill Cornell Medicine of Cornell University, New York, NY, USA

Abstract

Preoperative flexion contracture is a risk factor for patient dissatisfaction following primary total knee arthroplasty (TKA). Previous studies utilizing surgical navigation technology and cadaveric models attempted to identify operative techniques to correct knees with flexion contracture and minimize undesirable outcomes such as knee instability. However, no consensus has emerged on a surgical strategy to treat this clinical condition. Therefore, the purpose of this study was to develop and evaluate a computational model of TKA with flexion contracture that can be used to devise surgical strategies that restore knee extension and to understand factors that cause negative outcomes. We developed six computational models of knees implanted with a posteriorly stabilized TKA using a measured resection technique. We incorporated tensions in the collateral ligaments representative of those achieved in TKA using reference data from a cadaveric experiment and determined tensions in the posterior capsule elements in knees with flexion contracture by simulating a passive extension exam. Subject-specific extension moments were calculated and used to evaluate the amount of knee extension that would be restored after incrementally resecting the distal femur. Model predictions of the extension angle after resecting the distal femur by 2 and 4 mm were within 1.2° ($p \geq 0.32$) and 1.6° ($p \geq 0.25$), respectively, of previous studies. Accordingly, the presented computational method could be a credible surrogate to study the mechanical impact of flexion contracture in TKA and to evaluate its surgical treatment.

This is an open access article under the CC BY-NC-ND license (http://creativecommons.org/licenses/by-nc-nd/4.0/).

[*]Corresponding author at: 510 E 73rd St, New York, NY 10021, USA. elmasrys@hss.edu (S.S. Elmasry).

Conflict of Interest Statement

Michael Cross, Andrew Pearle, Timothy Wright, and Geoffrey Westrich are consultants and/or receive royalties with Exactech Inc.

Appendix A. Supplementary data

Supplementary data to this article can be found online at https://doi.org/10.1016/j.jbiomech.2021.110367.

Author Manuscript Author Manuscript Author Manuscript Author Manuscript

Keywords

Flexion contracture; Total Knee Arthroplasty; Passive extension moment; Ligament tension; Computational model; Additional resection of the distal femur

1. Introduction

Primary total knee arthroplasty (TKA) is largely successful in alleviating pain and improving patient function, but up to 15% of patients are dissatisfied with their surgical outcome (Gunaratne et al., 2017; Springer and Sotile, 2020; Yapp et al., 2020). Multiple risk factors for patient dissatisfaction have been described (Ghomrawi et al., 2020; Halawi et al., 2019; Springer and Sotile, 2020) including the improper correction of preoperative flexion contracture at surgery resulting in a postoperative flexion contracture (Koh et al., 2013; Tanzer and Miller, 1989). This complication leads to restricted range of motion, diminished knee function, and fatigue during standing, walking, and stair climbing (Anania et al., 2013; Bellemans et al., 2006; Koh et al., 2013).

Several surgical approaches have been utilized to correct preoperative flexion contracture during TKA, including intraoperative manipulation (Matsui et al., 2016), removal of posterior condylar osteophytes (Massin et al., 2009; Mihalko and Whiteside, 2003; Whiteside and Mihalko, 2002), release of the posterior capsule (Athwal et al., 2019; Okamoto et al., 2016), and additional distal femoral resection (Kim et al., 2017a; Liu et al., 2016). However, no consensus has emerged on a surgical strategy to restore the ability to achieve full extension. Previous studies utilizing navigation technology (Kim et al., 2017a; Liu et al., 2016) or cadaveric models (Cross et al., 2012) evaluated surgical techniques to achieve full extension and minimize undesirable outcomes such as knee instability. These clinical and cadaveric studies, however, lack the ability to precisely define important variables including the degree of flexion contracture, the amount of additional bone resection, or the level of ligament release while controlling for potential confounding factors such as variability in bony cuts, implant placement, and ligament properties. In contrast, computational models enable systematic comparison among surgical techniques while controlling for the effects of these confounding factors (Elmasry et al., 2020; Erdemir et al., 2019; Kia et al., 2018). A computational model incorporating ligament properties associated with preoperative flexion contracture would enable the study of different correction procedures to restore knee extension.

Therefore, the purpose of this study was to develop and evaluate a computational model of TKA with preoperative flexion contracture. The aims were, first, to incorporate tensions in the collateral ligaments representative of those achieved in mechanically aligned TKA with measured resection and posterior stabilized implants using reference data from a cadaveric experiment. Second, to determine tensions of the posterior capsule elements in a knee with flexion contracture by simulating a clinical exam of passive extension. Third, to quantify the amount of knee extension that would be restored by incrementally increasing the bone resection of the distal femur using the model. Finally, to compare model predictions to

Author Manuscript Author Manuscript Author Manuscript Author Manuscript

previously published clinical and cadaveric studies (Cross et al., 2012; Kim et al., 2017b; Liu et al., 2016).

2. Methods

Computational models derived from six cadaveric knees were virtually implanted with a PS TKA (Optetrak Logic®, Exactech, Gainesville, FL, USA) following our previously published framework (Elmasry et al., 2019, 2020; Kia et al., 2017, 2018). The model development pipeline included: segmenting and reconstructing the entire femoral and tibial bony geometries in 3D from computed tomography (CT) scans; creating bone-fixed and knee coordinate systems following the description of Grood and Suntay (1983); simulating bony cuts and implant positioning using measured resection and posterior referencing (Elmasry et al., 2019); incorporating ligament models that included the insertion locations and mean stiffnesses of the collateral and capsular structures (Kia et al., 2018); and adding a compliant contact formulation (Kia et al., 2017) (Supplementary material 1 and Fig. 1).

Our method of simulating flexion contracture in the TKA models consisted of five steps (Fig. 2): (1) measuring *in situ* collateral ligament forces in a cadaver knee after TKA implantation; (2) calibrating slack lengths of the medial and lateral collateral ligaments based on the ligament forces measured in the cadaver knee; (3) measuring tension in the posterior capsule by simulating a clinical exam of passive knee extension; (4) calibrating the slack length of the posterior capsule ligaments in the computational models to represent a knee with 10° of flexion contracture; and (5) simulating additional bone resection of the distal femur. A 10° flexion contracture was chosen because it is commonly observed in the clinic and to match the flexion angle used in a previous *in vitro* study (Cross et al., 2012). The increase in knee extension resulting from additional resection of the distal femur was then compared to data from previous *in vitro* experiments conducted by members of our research team and to clinical studies (Cross et al., 2012; Kim et al., 2017a; Liu et al., 2016).

In step one, a cadaveric experiment approved by our institutional review board was conducted to measure collateral ligament forces at full extension in a cadaver knee implanted with a TKA. A six-degrees-of-freedom robotic manipulator (ZX165U; Kawasaki Robotics, Wixom, MI) (Fig. 3) instrumented with a six-axis force-torque sensor (Theta; ATI, Apex, NC) (resolution: Fx = Fy = 0.13 N, Fz = 0.25 N, Tx = Ty = Tz = 0.008 Nm; limits: Fx = Fy = 1500 N, Fz = 3750 N, Tx = Ty = Tz = 240 Nm) was used to measure the forces applied to the knee joint (Imhauser et al., 2013). First, a PS TKA (LEGION, Smith & Nephew, Memphis, TN, USA) was installed on a pelvis-to-toe human cadaver (Male, 68 years old) using the measured resection technique by an experienced arthroplasty surgeon (co-author, MC) (Supplementary material 1). After installing the trial components, the surgeon conducted a standard clinical assessment of knee balance in extension and in flexion while visualizing the respective lateral and medial gaps at the knee joint. At full extension, the medial and lateral gaps were both estimated to be <1 mm. At 90° of flexion, the medial gap was estimated to be <1 mm and the lateral gap was <2 mm. After implant installation, the femoral and tibial diaphyses were cut 20 cm from the joint line. All soft tissues on the tibia and femur within 11 cm of the joint line were preserved. The fibula was then cut approximately 5 cm distal to its head/neck junction and was fixed proximally to the tibia

Author Manuscript Author Manuscript Author Manuscript Author Manuscript

using a wood screw. The exposed femur and tibia were then potted in bonding cement (Bondo, 3 M, St Paul, MN, USA). Subsequently, the femur was rigidly fixed to the ground through a pedestal and the potted tibia was fixed to the end effector of the robot with the knee in full extension. Anatomical axes were defined using a previously published registration technique (Camp et al., 2018; Imhauser et al., 2013). At full extension, the robot maintained a compressive force of 10 N while minimizing forces and torques in the remaining five directions to within 5 N and 0.4 Nm using a previously described algorithm (MATLAB; Mathworks, Natick, MA, USA) (Imhauser et al., 2013). Knee balance at full extension was confirmed using the industrial robot. Specifically, varus and valgus moments of ±6 Nm were applied to the knee and the resulting varus and valgus angulations were 0.7° and 1.6°, respectively. Finally, the superficial medial collateral ligament (MCL) and the lateral collateral ligament (LCL) were sectioned serially. The principle of superposition was used to measure *in situ* forces borne by each structure at full extension (Fujie et al., 1995).

In step two, six computational knee models were constructed based on cadaveric CT scans (Supplementary material 1). Twenty nonlinear springs representing eight ligaments were added to the tibiofemoral joint. Namely, the MCL, posterior oblique ligament (POL), LCL, anterolateral ligament (ALL), fabellofibular ligament (FFL), medial posterior capsule (PMC), and lateral posterior capsule (PLC), and oblique popliteal ligament (OPL) (Fig. 1). Ligament stiffnesses and insertion sites were defined using mean values from the literature and data from our previous studies (Elmasry et al., 2020; Kia et al., 2016). The slack lengths (l_0) of the MCL, POL, LCL, and FFL were calibrated to produce forces equal to those measured in cadaveric robotic experiments conducted in our laboratory. For the POL and FFL, forces measured in a native knee that was previously tested were utilized to calibrate their slack lengths (FFL: 1 N and POL: 18 N) (Kia et al., 2016). For the MCL and LCL, forces measured in the robotic experiment described above were targeted. A generalized reduced gradient optimization algorithm was utilized to minimize the differences between the resultant ligament forces predicted by the model (F_i^m) and those measured in the cadaveric experiments (F_i^e) at full extension (Eq. (1)) (Kia et al., 2016):

$$\min \sum_{i=1}^{4} \left(\left[\sum_{j=1}^{a} \left[\overrightarrow{F}_{i,j}^{m}(l, \dot{l}, l_0) \right]^2 \right]^{\frac{1}{2}} - F_i^e \right)^4 \tag{1}$$

a = total number of fibers comprising each of the 4 ligaments included in the optimization; i= ligament number; j= fiber number

$$F_i^m = \{sMCL, LCL, FFL, POL\}$$

$$F_i^e = \{45, 66, 1, 18\}\ N$$

$$a = \{6, 1, 1, 3\}\ fibers$$

Author Manuscript Author Manuscript Author Manuscript Author Manuscript

The ALL was observed to be slack at full extension; therefore, its slack length was increased by 15% of its length at full extension. At this stage, the slack lengths of the posterior capsule fibers comprising the PMC, PLC, and OPL were set equal to their fiber lengths at full extension prior to calibration in the next steps. The optimization was conducted with the knee fixed at full extension while allowing the tibia to move in the proximal–distal direction under 10 N of compression to resolve penetration of the articular surfaces. The remaining degrees of freedom were held constant.

In step three, a 2D static equilibrium model of a passive extension exam, which is commonly used to clinically evaluate flexion contracture, was generated to measure the knee extension moments (Fig. 4) (Bengs and Scott, 2006). The model represents a surgeon holding the foot of the patient at the heel with the toes pointing upward, the patient in a supine position, and their leg extending under the force of gravity. The force applied by the surgeon to lift the leg ($F_{surgeon}$) was measured using the moment equilibrium equation about the hip joint (Fig. 4a and Eq. (2)). The internal moment at the knee (M_{knee}) was measured using the moment equilibrium equation about the knee joint using the isolated foot and shank segment (Fig. 4b and Eq. (3)). Subject-specific measures of the weight and center of mass of the thigh, shank, and foot were estimated using anthropometric data and CT scans of each cadaveric leg (Table 1). The six subjects had body weights spanning those found in TKA patients (range: 511–1201 N). The center of mass of the thigh and shank were assumed to be distal to the center of the hip and knee joints by 41% and 45% of the length of the femur and tibia, respectively (De Leva, 1996). The weight of the thigh, shank, and foot were assumed to be 14.2%, 4.3%, and 1.4% of the bodyweight, respectively (De Leva, 1996).

$$\begin{aligned}\sum Moment \; = 0 - W_{Thigh} * (d_4 * \cos(30)) - W_{Shank}\,(d_3 * \cos(30) \\ + d_2 * \cos(20)) - W_{Foot}\,(d_3 * \cos(30) + d_1 * \cos(20)) \\ + F_{Surgeon} * (d_1 + d_3 * \cos(10)) = 0\end{aligned} \tag{2}$$

$$\begin{aligned}\sum \text{Moment} \; = 0 - M_{Knee} - W_{Foot} * (d_1 * \cos(20)) \\ - W_{Shank} * (d_2 * \cos(20)) + F_{Surgeon} * (d_1) = 0\end{aligned} \tag{3}$$

W_{Thigh}, W_{Shank}, and W_{Foot} represent the weights of the thigh, shank, and foot, respectively. $F_{surgeon}$ is the force applied by the surgeon to the foot and M_{knee} is the internal knee moment. d_1 is the shank length; d_2 is the distance between the shank center of mass and the knee joint; d_3 is the thigh length; and d_4 is the distance between the thigh center of mass and the hip joint.

In step four, the estimated subject-specific extension moments were applied to the six computational models at full extension (Fig. 5a). The magnitude of force carried by the posterior capsule (i.e., PMC, PLC, and OPL) to counterbalance this moment was recorded. Next, each knee model was flexed to 10° by rotating the femur by 10° about its medial–lateral axis while allowing the tibia five degrees of freedom (i.e., three translations, internal/external rotation, and varus/valgus rotation). With the knee fixed at 10° of flexion, the slack length of each component of the posterior capsule, l_0, was decreased to produce the forces required to resist the applied extension moments described in step three (Fig. 5b).

Author Manuscript Author Manuscript Author Manuscript Author Manuscript

Accordingly, a maximum passive extension of 10° was attained in the six models under the simulated passive extension exam.

Finally, in step five, a common surgical technique for treating flexion contracture was simulated by re-cutting the distal femur in increments of 2 and 4 mm (Fig. 5c) and keeping the tibial insert thickness constant. Each TKA model was then extended until the resultant force carried by the posterior capsule again equaled that of the tensioned capsule at the original 10° contracted position. The new flexion angle was measured after the two additional resections and compared to a previous cadaveric study performed by several members of our research team (Cross et al., 2012) and clinical data from the literature (Kim et al., 2017a; Liu et al., 2016). The statistical significance of the comparison was determined using a two-sample, two-tailed *t*-test ($p < 0.05$). Assuming a β of 20% and an α of 5%, a sample size of six provides adequate statistical power to detect an effect size of ≤1.27° compared to the previous studies (Cross et al., 2012; Kim et al., 2017a; Liu et al., 2016). Since these previous studies reported a change in extension angle between 3 and 4° after 2 and 4 mm of distal resection, an effect size of 1.27° was sufficient since it is at least 2.3 times less than the expected change in extension angle.

3. Results

The *in situ* forces carried by the MCL and LCL measured in the robotic experiment were 45 and 66 N, respectively. The predicted ligament forces (F_i^m) obtained after optimization of ligament slack were within 0.2 N of those measured in the cadaveric experiment (F_i^e) for the six computational models. The average slack lengths of each of the four ligaments, defined as a percentage of the fiber length at full extension (L_0/L_e), were 95.6% for the distal MCL, 95.3% for the proximal MCL, 93.3% for the LCL, 95.7% for the POL, and 99.9% for the FFL (Table 2).

The moments estimated in the passive extension exam for knees 1 through 6 were 9.4, 10.5, 7.6, 13.7, 5.5, and 8.7 Nm, respectively. The forces generated in the three capsular structures varied across the six knee models, ranging from 53 to 150 N in the PMC, from 31 to 111 N in the PLC, and from 49 to 125 N in the OPL (Table 3). The calibrated slack lengths, defined as a percentage of the fiber length at full extension (l_0/l_e), ranged from 66 to 79% in the PMC, from 76 to 81% in the PLC, and from 83 to 90% in the OPL (Table 3).

Resecting the distal femur by an additional 2 and 4 mm caused the knee models to achieve mean extension angles of 5.4 ± 0.6° and 1.7 ± 0.9°, respectively (Fig. 6). The mean predictions of the maximum extension angle after resecting the femur by 2 and 4 mm were within 1.2° ($p \geq 0.32$) and 1.6° ($p \geq 0.25$), respectively, of the mean extension angle reported in previous studies (Table 4).

4. Discussion

A new method of simulating flexion contracture in a computational model of TKA was presented. The method tuned the collateral ligaments and posterior capsule to be specific to patients with PS TKA who present with a 10° flexion contracture during a common clinical

Author Manuscript Author Manuscript Author Manuscript Author Manuscript

exam of passive extension. We found that the amount of extension gained by additional resection of the distal femur was in good agreement with the results of previous studies (Table 4). This finding suggests that the computational model is a credible surrogate to study flexion contracture in TKA and a tool to evaluate the mechanical impact of surgical approaches to treat this clinical condition.

The forces carried by the collateral ligaments following TKA vary depending on the bone resection technique, implant design, and whether ligament releases were performed (Elmasry et al., 2019; Kanamiya et al., 2002; Kia et al., 2018). Therefore, we carried out a robotic experiment using a cadaveric knee implanted with TKA to measure forces carried by the collateral ligaments at full extension in a knee with a PS TKA implanted using measured resection. The MCL (45 N) and LCL (66 N) carried higher forces than those previously reported for a native knee (MCL = 4 N and LCL = 20 N) (Kia et al., 2016). Surgeons often produce a soft tissue envelope that is tighter than the native knee in extension; thus, this finding is consistent with clinical practice (Shelton et al., 2019). Subsequently, in the six computational models, the calibrated slack lengths of the MCL and LCL were 95.6 and 93.3% of their respective lengths at full extension (Table 2). Calibrating ligament slack length to those of a knee following TKA is important because ligament forces are highly sensitive to this property (Cullen, 2014).

A clinical exam of passive knee extension is commonly used to evaluate the degree of flexion contracture (Bengs and Scott, 2006; Liu et al., 2016). Since passive extension depends on the weight and length of the leg (Fig. 4), we utilized six subjects with body weights that spanned those in typical TKA patients (range: 511–1201 N) (Table 1). This heterogeneity in each subject's weight yielded variability in both the applied subject-specific extension moments (range: 9.4–13.7 Nm) and the resulting decrease in the slack of the posterior capsule required to achieve a flexion contracture of 10°. This finding implies that surgeons should account for the mass and limb length of the patient when interpreting the degree of flexion contracture based on a passive extension exam. More specifically, a flexion contracture could be more severe (i.e., greater contraction) in heavier, taller patients than the same degree of contracture in a lighter, shorter patient.

In four out of the six models, the PMC carried the most force (ranging from 53 to 150 N) in response to subject-specific extension moments (Table 3). This finding emphasizes the role that each ligament plays in contracting the knee and is consistent with the common clinical practice of surgeons first releasing the medial aspect of the posterior capsule of the femur to increase knee extension (Chai et al., 2020; Scuderi and Kochhar, 2007). The slack length of the structures comprising the posterior capsule, namely the PMC, PLC, and OPL, decreased substantially (by 10–34%) relative to their respective lengths at full extension (Table 3). While the stiffness of the posterior capsule could also increase with flexion contracture, we could not generate the targeted contracture by only increasing the stiffness in our computational models. Thus, reduction in the resting length (i.e., slack length) of the capsular tissues is likely a major component of this common clinical entity.

The impact of resecting 2 and 4 mm of additional distal femur on maximum knee extension was consistent among the six knees (Fig. 6). In a cadaveric study by Cross et al. (2012), a

Author Manuscript Author Manuscript Author Manuscript Author Manuscript

10° flexion contracture was simulated by imbricating, via suturing, the posterior capsule. Additional distal femoral resection of 2 and 4 mm was performed and the mean maximal knee extension of 6.4° ± 2.5° and 1.4° ± 1.8° was achieved, respectively. In another study (Liu et al., 2016), spacer blocks were placed during a TKA, and the degree of knee flexion was measured with computer navigation. With 2, 4, and 6 mm block augments, a mean of 3.4°, 6.7°, and 11.4°, respectively, was observed. Finally, in a study of patients with a flexion contracture undergoing computer navigated TKA (Kim et al., 2017a), the measured mean change in flexion angle following 2 mm of additional resection was 4.8 ± 2.1°. The maximum difference between our model's prediction and these previous studies was 1.2° and 1.6° after the 2 and 4 mm of additional resection, respectively, with no significant difference ($p \geq 0.25$) (Table 4). Accordingly, our *in silico* model is comparable to *in vitro* and clinical models in simulating flexion contracture.

We acknowledge several limitations of our study. First, contracture of the posterior capsule was simulated in our computational models by altering the slack length of the elements representing the posterior capsule. However, posterior capsule contracture can also be attributed to ligament stiffening, the presence of osteophytes, or other subject-specific properties. It is unknown whether our method is valid for knees presenting with different contractures and/or different implants. Thus, our model only represents one possible mechanism for flexion contracture in TKA. Second, our methodology and results corroborated three previously published studies. Two of the three studies, however, used cruciate-retaining prosthesis (Kim et al., 2017a; Liu et al., 2016). Third, we did not simulate contraction of the collateral ligaments or other ligamentous structures in the knee that may contribute to a patient's flexion contracture because this study focused on contracture in the posterior capsule. Fourth, we defined collateral ligament tension in the six knee models based on experimental data of one well-balanced mechanically aligned knee. Intraoperative data show wide knee-to-knee variability in tibiofemoral contact forces in knees that were deemed balanced, which may indicate variation in collateral ligament tension (Elmallah et al., 2016). Therefore, our findings may not be representative of all possible ligament tensioning scenarios; sensitivity analyses should be used in the future to identify the impact of variable ligament tensioning on model predictions. Fifth, we utilized PS TKA; therefore, our results may not apply to TKA where the posterior cruciate ligament is preserved. Sixth, the PS implant system that was used in the cadaver experiment differed from the one that was used in the computational model. Since the implants have similar multi-radius designs and measured resection techniques were used to install each implant, the difference in ligament tensions is likely minimal. Finally, our model did not include a patellofemoral joint. Joint line elevation, due to additional femoral resection, may incur impingement of the patella against the tibial insert; a condition that may cause pain and flexion limitation (Bengs and Scott, 2006; Bong and Di Cesare, 2004). However, these conditions were correlated with joint line elevations >8 mm (Partington et al., 1999), which was not investigated in this study. Therefore, the effect of excluding the patellofemoral joint on the results of this study is likely minimal.

In conclusion, we developed computational models of TKA representing a knee with a flexion contracture of 10°. These models were informed by cadaveric measures of collateral ligament forces at full extension and a simulated clinical exam of passive extension. The

Author Manuscript Author Manuscript Author Manuscript Author Manuscript

predictions of the models corroborated passive extension angles measured in previous *in vitro* and clinical studies following additional distal femur resections. Accordingly, the computational method presented in this study could be a credible surrogate to evaluate the mechanical impact of flexion contracture and its surgical treatment in TKA.

Supplementary Material

Refer to Web version on PubMed Central for supplementary material.

Acknowledgments

The authors gratefully acknowledge Joseph Lipman, MS, for his contribution to this study. Shady Elmasry was supported by a training award from the National Center for Advancing Translational Sciences of the National Institutes of Health under Award Number TL1TR002386.

References

Anania A, Abdel MP, Lee Y-Y, Lyman S, Della Valle AG, 2013. The natural history of a newly developed flexion contracture following primary total knee arthroplasty. Int. Orthopaed 37, 1917–1923.

Athwal K, Milner P, Bellier G, Amis AA, 2019. Posterior capsular release is a biomechanically safe procedure to perform in total knee arthroplasty. Knee Surg Sports Traumatol Arthrosc 27, 1587–1594. [PubMed: 30094498]

Bellemans J, Vandenneucker H, Victor J, Vanlauwe J, 2006. Flexion contracture in total knee arthroplasty. Clin. Orthopaed. Related Res 452, 78–82.

Bengs BC, Scott RD, 2006. The effect of distal femoral resection on passive knee extension in posterior cruciate ligament–retaining total knee arthroplasty. J. Arthroplasty 21, 161–166. [PubMed: 16520201]

Bong MR, Di Cesare PE, 2004. Stiffness after total knee arthroplasty. J. Am. Acad. Orthopaedic Surg 12, 164–171.

Camp C, Jahandar H, Sinatro A, Imhauser C, Altchek D, Dines, 2018. Quantitative anatomic analysis of the medial ulnar collateral ligament complex of the elbow. Orthop. J. Sports Med 6, (3) 2325967118762751. [PubMed: 29637082]

Chai W, Chen Q-Q, Zhang Z, Shi L, Yan C-H, Guo R-W, Chen J-Y, 2020. Correcting severe flexion contracture with fusiform capsulectomy of posterior capsule during total knee arthroplasty. Int. Orthopaed, 1–6

Cross MB, Nam D, Plaskos C, Sherman SL, Lyman S, Pearle AD, Mayman DJJTK, 2012. Recutting the distal femur to increase maximal knee extension during TKA causes coronal plane laxity in mid-flexion. Knee 19, 875–879. [PubMed: 22727760]

Cullen M, 2014. Sensitivity Study of Knee Ligament Properties in a Computer Simulation of a Total Knee Arthroplasty. The Ohio State University.

De Leva P, 1996. Adjustments to Zatsiorsky-Seluyanov's segment inertia parameters. J. Biomech 29, 1223–1230. [PubMed: 8872282]

Elmallah RK, Mistry JB, Cherian JJ, Chughtai M, Bhave A, Roche MW, Mont MA, 2016. Can we really "feel" a balanced total knee arthroplasty?. J. Arthroplasty 31, 102–105. [PubMed: 27155994]

Elmasry SS, Imhauser CW, Wright TM, Pearle AD, Cross MB, Mayman DJ, Westrich GH, Sculco PK, 2019. Neither anterior nor posterior referencing consistently balances the flexion gap in measured resection total knee arthroplasty: a computational analysis. J. Arthroplasty 34, (981–986) e981.

Elmasry SS, Sculco PK, Kia M, Kahlenberg CA, Cross MB, Pearle AD, Mayman DJ, Wright TM, Westrich GH, Imhauser CW, 2020. A geometric ratio to predict the flexion gap in total knee arthroplasty. J. Orthopedic Res 38 (7) Special Issue: Recent Advances in Total Joint Replacement, 1637–1645.

Author Manuscript Author Manuscript Author Manuscript Author Manuscript

Erdemir A, Besier TF, Halloran JP, Imhauser CW, Laz PJ, Morrison TM, Shelburne KBJ, 2019. Deciphering the “art” in modeling and simulation of the knee joint: overall strategy. J. Biomech. Eng 141, (7) 071002.

Fujie H, Livesay GA, Woo SL, Kashiwaguchi S, Blomstrom G, 1995. The use of a universal force-moment sensor to determine in-situ forces in ligaments: a new methodology. J. Biomech. Eng 117, 1–7. [PubMed: 7609472]

Ghomrawi HM, Nwachukwu BU, Jain D, Wright T, Padgett D, Bozic KJ, Lyman S, 2020. Preoperative expectations associated with postoperative dissatisfaction after total knee arthroplasty: a cohort study. J. Am. Acad. Orthopaedic Surg 28, e145–e150.

Grood ES, Suntay WJ, 1983. A joint coordinate system for the clinical description of three-dimensional motions: application to the knee. J. Biomech. Eng 105, 136–144. [PubMed: 6865355]

Gunaratne R, Pratt DN, Banda J, Fick DP, Khan RJ, Robertson BWJ, 2017. Patient dissatisfaction following total knee arthroplasty: a systematic review of the literature. J. Arthroplasty 32, 3854–3860. [PubMed: 28844632]

Halawi MJ, Jongbloed W, Baron S, Savoy L, Williams VJ, Cote MP, 2019. Patient dissatisfaction after primary total joint arthroplasty: the patient perspective. J. Arthroplasty 34, 1093–1096. [PubMed: 30799270]

Imhauser C, Mauro C, Choi D, Rosenberg E, Mathew S, Nguyen J, Ma Y, Wickiewicz T, 2013. Abnormal tibiofemoral contact stress and its association with altered kinematics after center-center anterior cruciate ligament reconstruction: an in vitro study. Am. J. Sports Med 41, 815–825. [PubMed: 23470858]

Kanamiya T, Whiteside LA, Nakamura T, Mihalko WM, Steiger J, Naito M, 2002. Effect of Selective Lateral Ligament Release on Stability in Knee Arthroplasty. Clin. Orthop. Relat. Res 404, 24–31.

Kia M, Schafer K, Lipman J, Cross M, Mayman D, Pearle A, Wickiewicz T, Imhauser C, 2016. A multibody knee model corroborates subject-specific experimental measurements of low ligament forces and kinematic coupling during passive flexion. J. Biomech. Eng 138, 051010. [PubMed: 26926010]

Kia M, Warth LC, Lipman JD, Wright TM, Westrich GH, Cross MB, Mayman DJ, Pearle AD, Imhauser CW, 2017. Fixed-bearing medial unicompartmental knee arthroplasty restores neither the medial pivoting behavior nor the ligament forces of the intact knee in passive flexion. J. Orthop. Res, 1868–1875 [PubMed: 27935105]

Kia M, Wright TM, Cross MB, Mayman DJ, Pearle AD, Sculco P, Westrich GH, Imhauser CW, 2018. Femoral Component external rotation affects knee biomechanics: a computational model of posterior-stabilized TKA. Clin. Orthop. Relat. Res 476, 113–123. [PubMed: 29529625]

Kim SH, Lim J-W, Jung H-J, Lee H-J, 2017a. Influence of soft tissue balancing and distal femoral resection on flexion contracture in navigated total knee arthroplasty. Knee Surg. Sports Traumatol. Arthrosc 25, 3501–3507. [PubMed: 27539400]

Kim SH, Ro D-H, Cho Y, Lee Y-M, Lee S, Lee M-C, 2017b. What is the ideal degree of extension after primary total knee arthroplasty?. J. Arthroplasty 32, 2717–2724. [PubMed: 28487091]

Koh IJ, Chang CB, Kang YG, Seong SC, Kim TK, 2013. Incidence, predictors, and effects of residual flexion contracture on clinical outcomes of total knee arthroplasty. J. Arthroplasty 28, 585–590. [PubMed: 23142447]

Liu DW, Reidy JF, Beller EM, 2016. The effect of distal femoral resection on fixed flexion deformity in total knee arthroplasty. J. Arthroplasty 31, 98–102. [PubMed: 26321077]

Massin P, Petit A, Odri G, Ducellier F, Sabatier C, Lautridou C, Cappelli M, Hulet C, Canciani J, Letenneur J, 2009. Total knee arthroplasty in patients with greater than 20 degrees flexion contracture. Orthop Traumatol Surg Res 95, 7–12.

Matsui Y, Minoda Y, Fumiaki I, Nakagawa S, Okajima Y, Kobayashi A, 2016. Intraoperative manipulation for flexion contracture during total knee arthroplasty. Orthopedics 39, e1070–e1074. [PubMed: 27111075]

Mihalko WM, Whiteside LA, 2003. Bone resection and ligament treatment for flexion contracture in knee arthroplasty. Clin. Orthopaed. Related Res 406, 141–147.

Author Manuscript Author Manuscript Author Manuscript Author Manuscript

Okamoto Y, Nakajima M, Jotoku T, Otsuki S, Neo M, 2016. Capsular release around the intercondylar notch increases the extension gap in posterior-stabilized rotating-platform total knee arthroplasty. Knee 23, 730–735. [PubMed: 27174384]

Partington PF, Sawhney J, Rorabeck CH, Barrack RL, Moore J, 1999. Joint line restoration after revision total knee arthroplasty. Clin. Orthop. Relat. Res, 165–171.

Scuderi GR, Kochhar T, 2007. Management of flexion contracture in total knee arthroplasty. J. Arthroplasty 22, 20–24.

Shelton TJ, Howell SM, Hull ML, 2019. A total knee arthroplasty is stiffer when the intraoperative tibial force is greater than the native knee. J. Knee Surg. 32, 1008–1014. [PubMed: 30414168]

Springer BD, Sotile WM, 2020. The psychology of total joint arthroplasty. J. Arthroplasty 45, 46–49.

Tanzer M, Miller J, 1989. The natural history of flexion contracture in total knee arthroplasty. A prospective study. Clin. Orthopaed. Related Res, 129–134

Whiteside LA, Mihalko WM, 2002. Surgical procedure for flexion contracture and recurvatum in total knee arthroplasty. Clin. Orthopaed. Related Res 404, 189–195.

Yapp LZ, Clement ND, Macdonald DJ, Howie CR, Scott CE, 2020. Changes in expectation fulfilment following total knee arthroplasty: a 10-year follow-up study. J. Arthroplasty 35, 1826–1832. [PubMed: 32205005]

Author Manuscript Author Manuscript Author Manuscript Author Manuscript

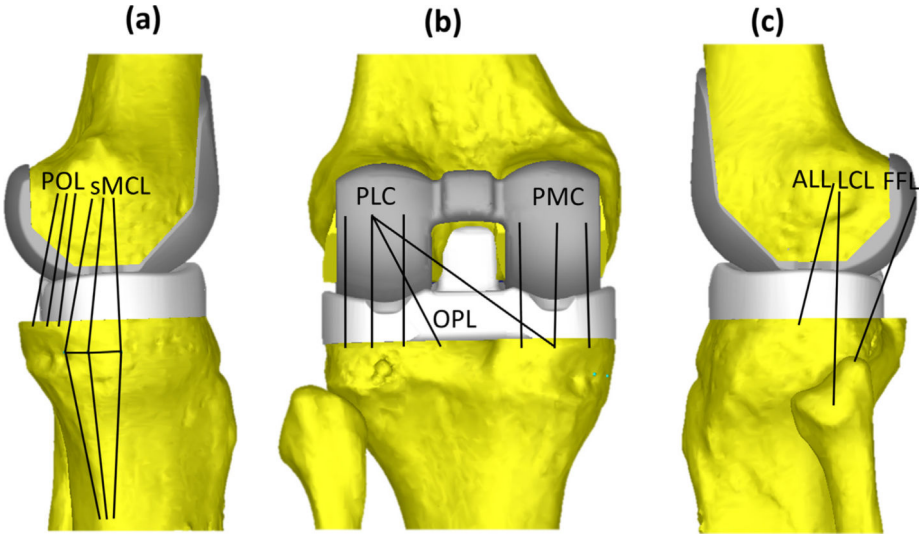

Fig. 1.

A computational model of a posterior stabilized total knee arthroplasty that was developed using the pipeline described in Supplementary material 1. The model included a total of 20 ligament fibers representing the collateral ligaments and posterior capsule: (a) Medial ligaments, (b) Posterior capsule, and (c) Lateral ligaments. PMC: medial posterior capsule, PLC: lateral posterior capsule, OPL: oblique popliteal ligament, LCL: lateral collateral ligament, ALL: anterolateral ligament, FFL: fabellofibular ligament, MCL: superficial medial collateral ligament, POL: posterior oblique ligament.

Author Manuscript Author Manuscript Author Manuscript Author Manuscript

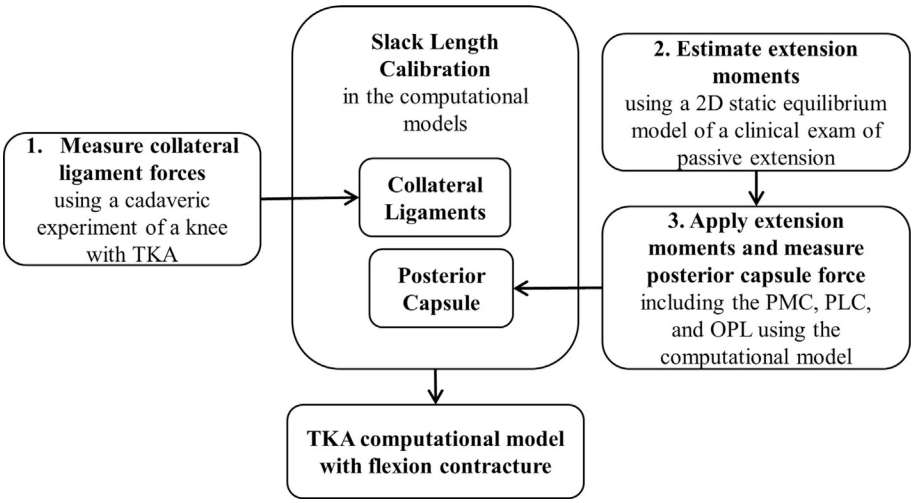

Fig. 2.

Flow chart demonstrating the steps used to calibrate the slack lengths of the collateral ligaments and posterior capsule in the computational model of total knee arthroplast (TKA) with flexion contracture. PMC: posterior medial capsule; PLC: posterior lateral capsule; OPL: oblique popliteal ligament.

Author Manuscript Author Manuscript Author Manuscript Author Manuscript

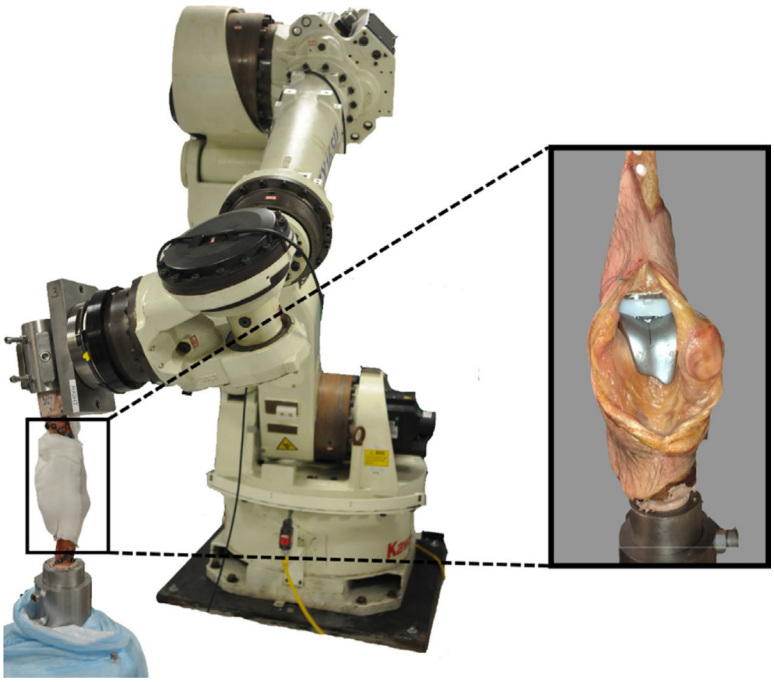

Fig. 3.

Image of the six-degrees-of-freedom robot and a cadaveric knee implanted with total knee arthroplasty. The knee is mounted to the robot at full extension. The robot is instrumented with a six-axis force-torque sensor.

Author Manuscript Author Manuscript Author Manuscript Author Manuscript

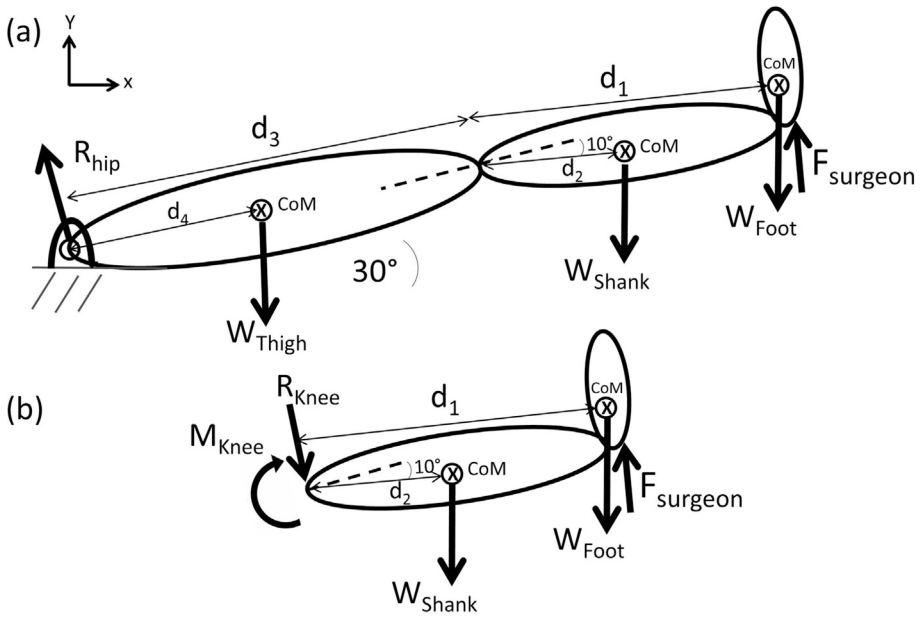

Fig. 4.

Two-dimensional free body diagrams representing the clinical exam of passive extension. (a) Diagram of the full leg to determine the force applied by the surgeon to lift the foot. (b) Diagram of the shank and foot segments to determine the internal moment at the knee. Rhip: reaction force at the hip; W_{Thigh}: thigh weight, W_{Shank}: shank weight; W_{Foot}: foot weight; and $F_{surgeon}$: surgeon lifting force; d_1: shank length; d_2: distance from the center of the knee joint to the center of mass of the shank; d_3: thigh length, d_4: distance from the center of the hip joint to the center of mass of the thigh; CoM: center of mass.

Author Manuscript Author Manuscript Author Manuscript Author Manuscript

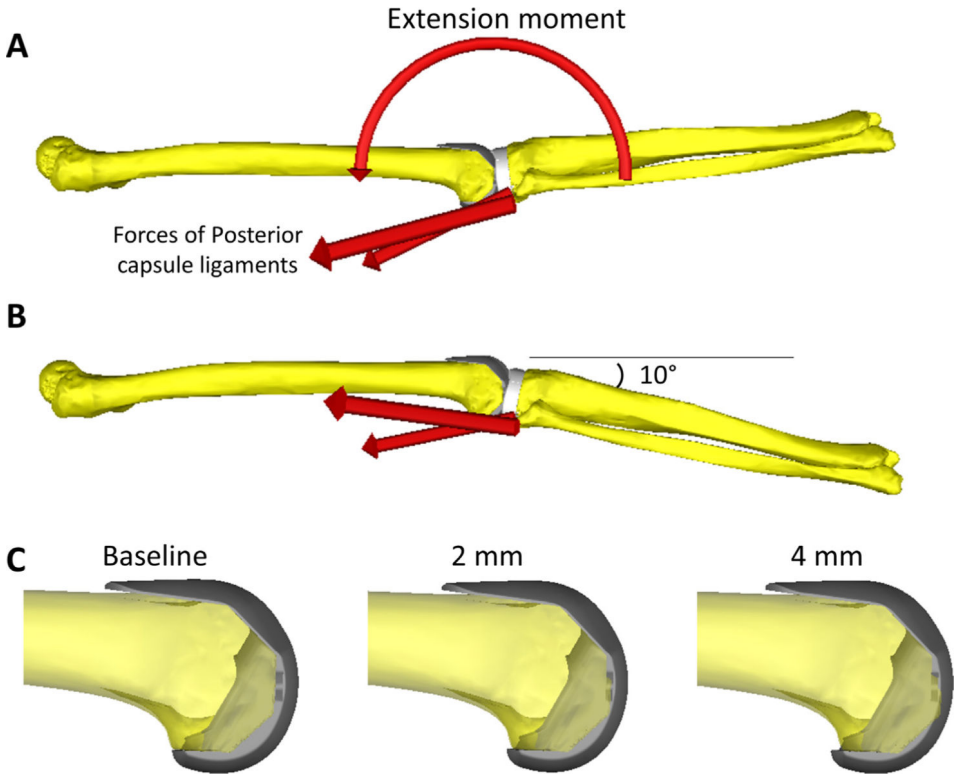

Fig. 5.

Methods used to simulate a 10° flexion contracture in the computational model. A. applying an extension moment to the knee joint to estimate the reaction forces in the elements representing the posterior capsule; B. flexing the knee by 10° and calibrating the slack length of the posterior capsule ligaments to generate the forces estimated in A; C. proximalizing the femoral component to simulate additional 2 and 4 mm distal femoral resection relative to the baseline position.

Author Manuscript Author Manuscript Author Manuscript Author Manuscript

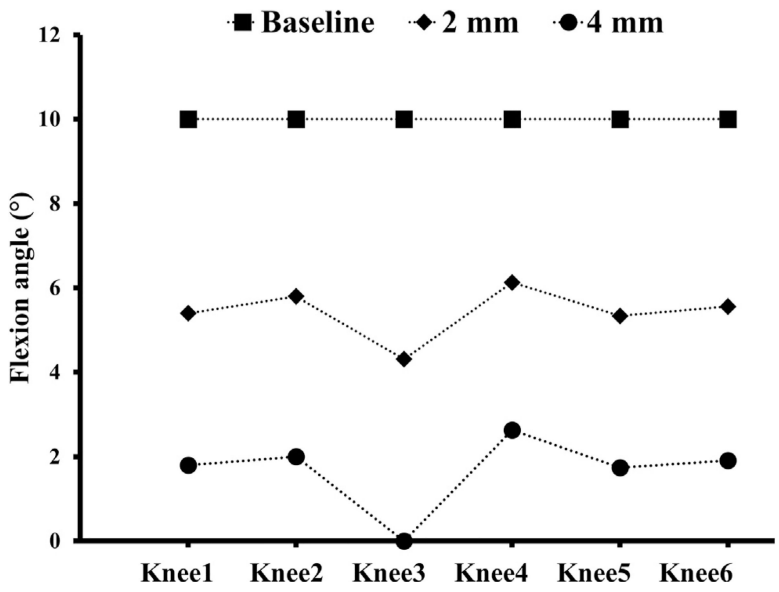

Fig. 6.

The flexion angle at baseline and following 2 and 4 mm of additional distal femoral resection for the six knee models.

Author Manuscript Author Manuscript Author Manuscript Author Manuscript

Table 1

Anthropometric measures of the six cadaveric legs from which the computational knee models were developed.

	Knee 1	Knee 2	Knee 3	Knee 4	Knee 5	Knee 6
Body Weight (N)	778	823	667	1201	511	756
Femur length d_3 (mm)	485	508	467	460	428	467
Tibia length d_1 (mm)	408	440	370	382	362	372
Thigh weight (N)	110.2	116.5	94.4	170.1	72.4	107.0
Shank weight (N)	33.7	35.6	28.9	52.0	22.1	32.7
Foot weight (N)	10.7	11.3	9.1	16.5	7.0	10.4
d_4 (mm)	199	208	191	189	175	191
d_2 (mm)	184	198	167	172	163	167

N= Newton; mm= millimeter; d_4= distance from hip joint center to thigh center of mass; d_2= distance from knee joint center to shank center of mass.

Author Manuscript Author Manuscript Author Manuscript Author Manuscript

Table 2

The mean and standard deviation (SD) of the slack length (l_0) of ligament fibers in the six knee models calculated as a percentage (l_0/l_e (%)) of the fiber length at full extension (l_e) after calibration.

		l_e (mm)		l_0/l_e (%)		l_0 (mm)	
Ligament	**Ligament fiber**	**Mean**	**SD**	**Mean**	**SD**	**Mean**	**SD**
MCL	**MCL distal$_1$**	44.1	3.2	95.6	1.2	42.2	3.1
	MCL distal$_2$	44.0	3.7	95.6	1.2	42.1	3.7
	MCL distal$_3$	43.9	3.4	95.6	1.2	42.0	3.4
	MCL proximal$_1$	40.2	3.9	95.3	1.4	38.3	3.4
	MCL proximal$_2$	41.6	4.6	95.3	1.4	39.6	4.1
	MCL proximal$_3$	41.0	4.5	95.3	1.4	39.0	4.0
LCL		60.6	6.1	93.3	5.1	56.4	3.3
POL	**POL$_1$**	39.0	4.5	95.7	2.1	37.3	4.9
	POL$_2$	38.9	4.0	95.7	2.1	37.3	4.5
	POL$_3$	40.0	4.4	95.7	2.1	38.3	4.9
FFL		45.1	6.1	99.3	1.5	44.7	5.7

MCL: medial collateral ligament, LCL: lateral collateral ligament, POL: posterior oblique ligament, and FFL: fabellofibular ligament. For the MCL and POL, fibers 1 to 3 are numbered from anterior to posterior.

J Biomech. Author manuscript; available in PMC 2021 June 07.

Author Manuscript Author Manuscript Author Manuscript Author Manuscript

Table 3

Calculated forces and slack lengths of the structures comprising the posterior capsule PMC (posteromedial capsule), PLC (posterolateral capsule), and OPL (oblique popliteal ligament) after they were calibrated in the six knee models.

	Knee 1		Knee 2		Knee 3		Knee 4		Knee 5		Knee 6	
	Force (N)	**(l_0/l_e) %**	**Force (N)**	**(l_0/l_e) %**	**Force (N)**	**(l_0/l_e) %**	**Force (N)**	**(l_0/l_e) %**	**Force (N)**	**(l_0/l_e) %**	**Force (N)**	**(l_0/l_e) %**
PMC	95	70.1	142	66.1	69	69.2	150	71.8	53	79.0	84	77.0
PLC	77	78.3	46	76.7	111	79.7	95	74.6	31	81.2	58	80.3
OPL	72	83.0	61	88.2	49	89.0	125	86.3	63	90.1	62	90.2

l_0 = ligament slack length; l_e = ligament length at full extension

Author Manuscript Author Manuscript Author Manuscript Author Manuscript

Table 4

Mean ± SD increase in knee extension after recutting the distal femur by an additional 2 and 4 mm of our knee models compared to three previously published studies.

	Increase in Knee Extension (°)			
	2 mm	**P value**	**4 mm**	**P value**
Knee models	4.6° ± 0.6°		8.3° ± 0.9°	
Cross 2012 [18]	3.6° ± 2.5°	0.36	8.6° ± 1.8°	0.72
Liu 2016 [16]	3.4° ± 2.9	0.32	6.7° ± 3.1	0.25
Kim 2017 [17]	4.8° ± 2.1	0.82	–	

J Biomech. Author manuscript; available in PMC 2021 June 07.